# Direct Computation of Static Difference Magnetic Field in Nonlinear Magnetic Materials and Application to Shape Reconstruction of Damaged Areas in Aging Materials

Bogdan Cranganu-Cretu, Florea Ioan Hantila, Gabriel Preda, Zhenmao Chen, and Kenzo Miya

***Abstract*—In order to accurately compute the magnetic field variation due to changes in material properties (e.g., material aging) we propose a technique that computes directly the difference magnetic field. Nonlinear materials are analyzed by means of the polarization technique. The linear field problem is solved using a fast Green function approach. A two-dimensional formulation is validated upon comparison with measurement data. Then, it is used as fast forward solver for a neural network approach to the inverse problem of reconstructing the shape of the aged material area in a plate. Finally, results of reconstruction, based on 500 cases database simulations of a yoke and plate geometry, are presented pointing out good quality of the reconstruction.**

***Index Terms*—Magnetic fields, neural networks, nondestructive testing, nonlinear magnetics.**

## I. Introduction

A RANGE of nondestructive testing techniques has been fostered as the subject of nondestructive evaluation (NDE) assumed an ever increasing role prompted by numerous industries—among which nuclear power plants and gas facilities—becoming aware of the urge for plant life extension or avoiding catastrophic failures by monitoring the condition of structures for both defect appearance and material degradation [1].

When ferromagnetic materials are investigated, magnetic methods [1] as magnetic flux leakage testing (MFLT) are best fitted. The presence of a defect in a magnetized ferromagnetic material results in a redistribution of magnetic field, leaking in the surrounding medium, which can be detected to measure the magnetic flux density $\mathbf{B}$ [2]. Applications of such method to pipe lines inspection are reported in [2], [3]. Solving the electromagnetic field problem, given the geometry and material characteristics is known as solving the direct problem, whilst inferring the geometry of the affected area from the measured signal is known as inverse analysis.

Regarding the direct problem, as small changes in magnetic properties are prompting to rather small changes in magnetic field distribution, computing flawed and unflawed signals may result in erroneous numerical results. In this paper, we are presenting an interesting approach allowing for the direct computation of the change in the magnetic field. The linear field problem—obtained upon use of polarization method [4]—is solved by means of a Green function approach. The advantages of such an approach were pointed as early as [5].

As for the inverse problem, many approaches were based on the analysis of underlying physical process in the so-called *model-based* methods [6]–[8]. Problems related to complexity, or low speed of the solution in these attempts have suggested that *model-free* approaches could represent a good candidate to be used in hybrid or standalone schemes. Moreover, relying on a pre-stored database, a model-free inversion possesses an increased independence to the employed numerical model, thus making more approachable the estimation of real cracks. Successful attempts based on neural network applications were presented in [9]–[12]. Lately, the use of genetic algorithm for inversion is gaining momentum as prompted by application [13], [14] but the area is, in our opinion, yet to be explored.

In this paper, we use a neural network approach combined with a module of statistical analysis of the data to infer the shape of the damaged area from the field signals previously computed.

## II. Magnetic Field Problem Formulation

In domain $\Omega$ the magnetic field verifies the following equations:

$$\nabla \times \mathbf{H} = \mathbf{J} \tag{1}$$

$$\nabla \mathbf{B} = 0 \tag{2}$$

$$\mathbf{H} = \hat{\mathbf{F}}(\mathbf{B}). \tag{3}$$

Nonlinear function $\hat{\mathbf{F}}$: $L^2(\Omega) \rightarrow L^2(\Omega)$ refers to the domains with ferromagnetic bodies and permanent magnets.

Manuscript received July 5, 2001; revised October 25, 2001.

B. Cranganu-Cretu was with the International Institute of Universality, Tokyo 113-0031, Japan. He is now with the Department of Electrical Engineering, Politehnica University of Bucharest, Bucharest 77206, Romania (e-mail: bogdan@elth.pub.ro).

F. I. Hantila is with the Department of Electrical Engineering, Politehnica University of Bucharest, Bucharest 77206, Romania (e-mail: hantila@elth.pub.ro).

Z. Chen, G. Preda, and K. Miya were with Tokyo University, Japan. They are now with International Institute of Universality, Tokyo 113-0031, Japan (e-mail: preda@jsaem.gr.jp; miya@jsaem.gr.jp).

Publisher Item Identifier S 0018-9464(02)01260-8.

### A. Polarization Method

The nonlinear field problem starts by replacing the constitutive relation in (3) with

$$\mathbf{B} = \mu\mathbf{H} + \mathbf{I} \tag{4}$$

in which the nonlinearity is hidden [4] in the polarization $\mathbf{I}$

$$\mathbf{I} = \mathbf{B} - \mu \cdot \hat{\mathbf{F}}(\mathbf{B}) = \hat{\mathbf{G}}(\mathbf{B}). \tag{5}$$

The local form of previous relation is

$$\mathbf{I} = \mathbf{B} - \mu \cdot \boldsymbol{f}(\mathbf{B}) = \boldsymbol{g}(\mathbf{B}). \tag{6}$$

The iterative convergent algorithm [4] goes as follows:

1) an arbitrary value $\mathbf{I}^{(0)}$ is given;
2) magnetic field $(\mathbf{B}^{(n)}, \mathbf{H}^{(n)})$ is computed, which verifies:

$$\nabla \times \mathbf{H}^{(n)} = \mathbf{J}, \qquad \nabla \mathbf{B}^{(n)} = 0, \qquad \mathbf{B}^{(n)} = \mu\mathbf{H}^{(n)} + \mathbf{I}^{(n-1)};$$

3) $\mathbf{I}^{(n)}$ is corrected according to (5): $\mathbf{I}^{(n)} = \hat{\mathbf{G}}(\mathbf{B}^{(n)})$.

Steps 2) and 3) are repeated until an imposed error limit is attained [1]

$$\left\| \mathbf{I}^{(n)} - \mathbf{I}^{(n-1)} \right\|_{L^2(\Omega)} = \sqrt{\nu \left( \mathbf{I}^{(n)} - \mathbf{I}^{(n-1)} \right)^2 d\Omega} \leq \varepsilon. \tag{7}$$

The procedure's linear convergence is considerably improved by using overrelaxation technique [4].

### B. Linear Field Problem

For the integral approach proposed here to solve the linear field problem, we consider that $\Omega$ is the whole space $R^2$ and the working permeability in (3) is imposed to be $\mu_0$—in all ferromagnetic subdomains. The ferromagnetic regions are divided into a number of $n_f$ subdomains denoted by $\omega_i$, having constant polarization $\mathbf{I}$ values. In each subdomain the flux density is

$$\mathbf{B}_i = \mathbf{B}_J + \tilde{\mathbf{B}}_i \tag{8}$$

where $\mathbf{B}_0$ is given by the current density (which is constant in subdomains $\gamma_k$)

$$\mathbf{B}_J = -\frac{\mu_0}{2\pi} \sum_{k=1}^{n_J} J_k \oint_{\partial\gamma_k} \ln R \, d\mathbf{l} = \sum_{k=1}^{n_J} \mathbf{u}_{ik} J_k. \tag{9}$$

$\mathbf{B}_o$ is computed only once before the iterations. $\tilde{\mathbf{B}}_i$ is the average value of the flux density given by polarization $\mathbf{I}$ [15]

$$\tilde{\mathbf{B}}_i = \frac{1}{\sigma(\omega_i)} \int_{\omega_i} \mathbf{B} \, dS = \left[ \frac{-1}{2\pi\sigma(\omega_i)} \right] \cdot \sum_{k=1}^{n_f} \oint_{\partial\omega_k} \oint_{\partial\omega_i} \ln R(\mathbf{I}_k \, d\mathbf{l}_k) \, d\mathbf{l}_i = \frac{-1}{\sigma(\omega_i)} \sum_{k=1}^{n_f} \overline{\overline{\alpha}}_{ik} \mathbf{I}_k \tag{10}$$

where

$$\overline{\overline{\alpha}}_{ik} = \frac{1}{2\pi} \oint_{\partial\omega_k} \oint_{\partial\omega_i} \ln R \, d\mathbf{l}_k; \qquad d\mathbf{l}_i \tag{11}$$

where ";" is the dyadic product.

### C. The Difference Magnetic Field

Upon computation of the magnetic field $(\mathbf{B}_0, \mathbf{H}_0)$ in the unflawed configuration, polarization $\mathbf{I}_0$ is obtained in all ferromagnetic subdomains as satisfying

$$\begin{aligned} \nabla \times \mathbf{H}_0 &= \mathbf{J} \\ \nabla \mathbf{B}_0 &= 0 \end{aligned} \tag{12}$$

$$\mathbf{B}_0 = \begin{cases} \mu_0 \mathbf{H}_0 + \hat{\mathbf{G}}(\mathbf{B}_0), & \text{in ferromag tic subdomains;} \\ \mu_0 \mathbf{H}_0, & \text{in air.} \end{cases}$$

For a small variation of the constitutive relation from $\hat{\mathbf{F}}$ to $\hat{\mathbf{F}}'$, the difference $(\Delta\mathbf{B}, \Delta\mathbf{H}) = (\mathbf{B}, \mathbf{H}) - (\mathbf{B}_0, \mathbf{H}_0)$ of the magnetic fields verifies (13)

$$\begin{aligned} \nabla \times \Delta\mathbf{H} &= 0 \\ \nabla \Delta\mathbf{B} &= 0 \end{aligned} \tag{13}$$

$$\Delta\mathbf{B} = \begin{cases} \mu_0 \Delta\mathbf{H} + \Delta\mathbf{I}, & \text{with } \Delta\mathbf{I} = \left. \dfrac{d\hat{\mathbf{G}}'}{d\mathbf{B}} \right|_{\mathbf{B}_0} (\Delta\mathbf{B}) \\ & \quad + \mu_0 \left( \hat{\mathbf{G}}'(\mathbf{B}_0) - \hat{\mathbf{G}}(\mathbf{B}_0) \right) \\ & \quad \text{in ferromagnetic subdomains;} \\ \mu_0 \Delta\mathbf{H}, & \text{in air} \end{cases}$$

where $\mathbf{G}'$ is defined by (5). The Frechet derivative $d\hat{\mathbf{G}}/d\mathbf{B}$ results from Frechet derivative of the local function $\boldsymbol{g}$. For example, in a homogeneous medium we have

$$\frac{d\boldsymbol{g}}{d\mathbf{B}} = \frac{1}{B^2} \frac{dg}{dB} (\mathbf{B}; \mathbf{B}) + \frac{g(B)}{B} \overline{\overline{\mathbf{1}}} - \frac{g(B)}{B^3} (\mathbf{B}; \mathbf{B}). \tag{14}$$

Since the aging material exhibiting modified material law is modeled as elements with different magnetic characteristic, the coefficients of polarization (11) do not change.

## III. Shape Reconstruction of Aged Material Area—Inverse Procedure

The problem of detecting and evaluating areas with aged material is important in nondestructive testing. In the following application, we assume knowledge of the modified constitutive relation and aim to reconstruct the shape of the aged material area in a plate sample. The above field computation procedure is used as the forward (or direct) solver of our problem.

The inverse problem aims to discover the signal-to-shape relationship existing between the simulated field signal and the geometry of the aged area by means of a neural network (*NN*) application. It has been noticed that *NN* learning algorithms often ignore much of the information contained in the data and, therefore, the preprocessing of the training data may improve the conditioning of the problem. This is realized by the combination of two modules [16]: the statistical analysis and transformation of the input data [by principal component analysis (PCA)], and the *NN* with incremental-resolution learning [17]. The procedure used is extensively described in [9], [16]. The neural network contains a single hidden layer along with direct connections between inputs and outputs to account for mapping linearities. The training starts with only one hidden node, and for each training epoch a new node is created, the new input-hidden connections

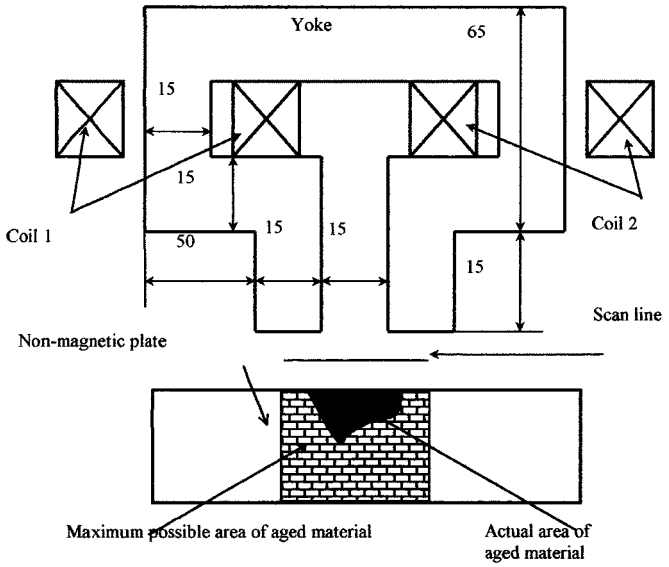


Fig. 1. Experimental setup (all dimensions in millimeters).

receive random weights, and the rest of the weights are solved by a least-square minimization using singular value decomposition. The PCA and *NN* modules are presented with the training data and issue two files for later use. The PCA file is used for the transformation of both the validation, and verification sets. The validation set is used only to control the training optimality, by monitoring the currently achieved estimation error. The reconstructions are conducted on the verification set, and, if available, the corresponding "correct" shapes are compared with the estimated ones. The latter set is the equivalent to the *on site* scan data. At this stage, the previously recorded files are employed, and only elementary operations are necessary for data transformation and propagation through the trained network. These two steps are very fast and can be performed even in real-time with small computation requirements during the actual testing. Being based on learning an input–output mapping from a set of examples (the training set) or fitting in a least-squares sense a hypersurface to this set in view of acquiring good generalization properties in unpopulated points, the whole procedure is equivalent to a statistical regression.

## IV. Numerical Results

In a first step, the results of the above numerical field computation procedure were confronted with experimental data. The problem configuration is presented in Fig. 1. It is a typical setup for a MFL inspection. The coils have cross section $33 \times 35$ mm each, current in each coil being 70 AT. Yoke nonlinear material was pure iron. Results for comparison of $B_z$ component of the field are shown in Fig. 2. The comparison was done in the case of a linear material in the plate. For the reconstruction case, we simulated a geometry consisting of a plate energized by a U-shaped yoke. The yoke-plate air gap was 0.1 mm. In our simulation, we focus on a reduced area where the material law may change, due to the aging process (as in Fig. 3). Inside this area, a randomly distributed zone—corresponding to the aged material—was simulated having a modified magnetic characteristic (Fig. 3).

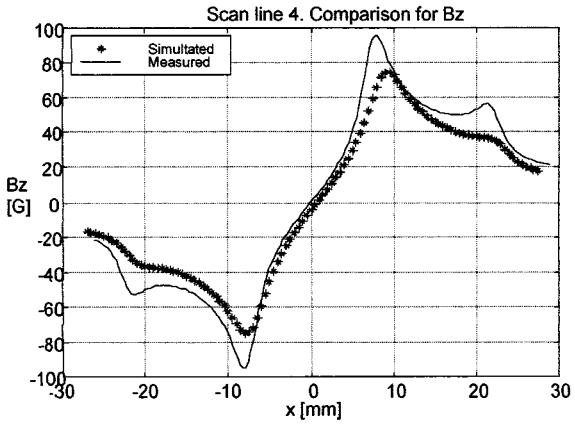


Fig. 2. Experiment versus simulation comparison of $Bz$.

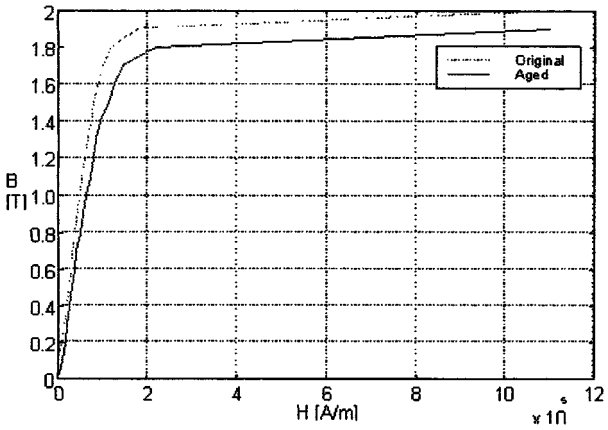


Fig. 3. Original and aged material constitutive relation.

A scan line was considered, 1.8 mm above the plate, and 20 readings were simulated on a 20-mm length spanning the maximum possible length of the aged area. The aged area was considered in an inner position (similar to an ID).

The mesh used for the two-dimensional forward procedure was 1998 elements and 2108 nodes. A total of 500 cases were generated. The database was divided into a training set (330 cases), a validation set (150 cases) and a verification set (20 cases). The training was stopped after 250 epochs with best reconstruction obtained for 40 epoch. In Fig. 4, four reconstruction examples are presented in gray-level images. We consider that given the relatively reduced dimension of the database and the huge dimension of the space of possible configurations the quality of the results we are presenting proves the usefulness of our approach.

The main time-consuming step in our approach is the establishment of the database of cases. For the application presented in this paper, a case (one configuration of damaged area) was solved in 35 s—so total time 4 h 30 min on a PC with Pentium III at 500 MHz. The actual process of *NN* training took 35 min. Once the training is achieved, feeding data to the *NN* results in extremely fast processing. The authors are also considering the extension of the field solution procedure to the three-dimensional case. As we choose the working permeability to be $\mu_0$, we are dealing with the whole space for which the Green function is available. The difficulty lays in the numerical computational effort which will considerably increase.

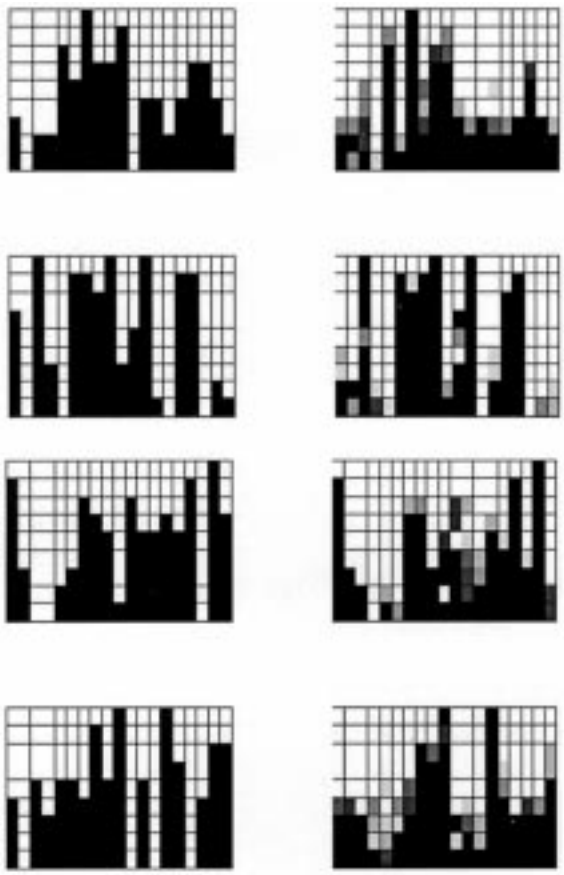

Fig. 4. Original and reconstructed shape of aged area (white-aged area).

## V. Conclusion

In this paper, we have presented a direct approach to computing the difference magnetic field appearing in the situation of a slight change in the magnetic characteristic. The field problem is first linearized by means of polarization method and then solved using a Green function approach. This procedure is then used as direct solver for the inverse problem based on an *NN* application aiming at inferring the shape of aged material from the magnetic field simulated for a plate configuration. Comparisons with measurement data showed good results of forward solver, whilst the results of reconstruction prove the feasibility of the method.

## References


[1] D. C. Jiles, "Review of magnetic methods for nondestructive evaluation," *NDT Int.*, vol. 21, pp. 311–319, May 1988.

[2] G. Katragadda, W. Lord, Y. S. Sun, S. Udpa, and L. Udpa, "Alternative magnetic flux leakage modalities for pipeline inspection," *IEEE Trans. Magn.*, vol. 32, pp. 1581–1585, May 1996.

[3] S. Leonard and D. L. Atherton, "Calculations of the effects of anisotropy on magnetic flux leakeage detector signals," *IEEE Trans. Magn.*, vol. 32, pp. 1905–1909, May 1996.

[4] I. F. Hantila, G. Preda, and M. Vasiliu, "Polarization method for static fields," *IEEE Trans. Magn.*, vol. 36, pp. 672–675, July 2000.

[5] L. Udpa and W. Lord, "A discussion of the inverse problem in electromagnetic NDT," in *Review on Progress in Quantitative Nondestructive Evaluation*, D. O. Thomson and D. E. Chimenti, Eds. New York: Plenum, 1990, vol. 5A, pp. 375–382.

[6] H. Igarashi, T. Honma, and A. Kost, "Inverse inference of magnetization distribution in cylindrical permanent magnets," *IEEE Trans. Magn.*, vol. 36, pp. 1168–1171, July 2000.

[7] T. Takagi, H. Huang, H. Fukutomi, and J. Tani, "Numerical simulation of correlation between crack size and eddy current testing signal by a very fast simulator," *IEEE Trans. Magn.*, vol. 34, pp. 2581–2584, May 1998.

[8] Z. Chen and K. Miya, "ECT inversion using a knowledge-based forward solver," *J. Nondestr. Eval.*, vol. 17, pp. 167–175, Mar. 1998.

[9] G. Preda, R. C. Popa, K. Demachi, and K. Miya, "Inverse mapping in ECT based on a shifting aperture approach and neural network regression," in *Proc. IJCN'99*, Washington, DC, July 10–16, 1999, pp. 4033–4036.

[10] R. Albanese *et al.*, "Analysis of metallic tubes with ECT and neuro-fuzzy processing," *Int. J. Appl. Electromagn. Mech.*, vol. 9, pp. 325–338, 1998.

[11] N. Yusa, W. Cheng, and K. Miya, "Inverse problems in eddy current testing using neural networks," in *Review on Progress in Quantitative Nondestructive Evaluation*, D. O. Thomson and D. Chimenti, Eds. New York: Plenum, 1999, vol. 19A, pp. 549–556.

[12] P. Ramuhall, L. Udpa, and S. Udpa, "Neural network algorithm for electromagnetic NDE signal inversion," in *Review on Progress in Quantitative Nondestructive Evaluation*, J. Pavo, Ed. New York: Plenum, 2001, vol. V, pp. 121–128.

[13] F. Zaoui, C. Marchand, and J. Pavo, "Stochastic crack inversion by an integral approach," in *Review on Progress in Quantitative Nondestructive Evaluation*, J. Pavo, Ed. New York: Plenum, 2001, vol. V, pp. 129–136.

[14] N. Yusa and K. Miya, "Inversion of eddy current NDE signals using genetic algorithm," *JSAEM Stud. App. Electromagn. Mech.*, vol. 9, pp. 619–620, 2001.

[15] I. F. Hantila, C. Mihai, E. Demeter, and R. Vasile, "Sensitivities in electrical machines," *JSAEM Stud. App. Electromagn. Mech.*, vol. 8, pp. 215–220, 1999.

[16] R. C. Popa and K. Miya, "Approximate inverse mapping in ECT, based on aperture shifting and neural network regression," *J. Nondestr. Eval.*, vol. 17, pp. 209–221, Apr. 1998.

[17] C. L. P. Chen, "A rapid supervised learning neural network for function interpolation and approximation," *IEEE Trans Neural Networks*, vol. 7, pp. 1220–1230, June 1996.